Supporting Information

Soil emissions, soil air dynamics and model simulation of gaseous mercury in subtropical forest

Jun Zhou [a, b, c], Zhangwei Wang [a, b, *], Xiaoshan Zhang [a, b], Charles T. Driscoll [d], Che-Jen Lin [e]

a. Research Center for Eco-Environmental Sciences, Chinese Academy of Sciences, Beijing 100085, China

b. University of Chinese Academy of Sciences, Beijing 100049, China.

c. Key Laboratory of Soil Environment and Pollution Remediation, Institute of Soil Science, Chinese Academy of Sciences, Nanjing 210008, China

d. Department of Civil and Environmental Engineering, Syracuse University, 151 Link Hall, Syracuse, New York 13244, United States

e. Center for Advances in Water and Air Quality, Lamar University, Beaumont, Texas 77710, United States

* Corresponding author: Zhangwei Wang.

E-mail address: wangzhw@rcees.ac.cn(Z. Wang); Phone: +86 10 62849168.

No.18 Shuangqing Road, Beijing 100085, China

First author e-mail: zhoujun@issas.ac.cn (J. Zhou).

Contents:

20 Pages

4 Tables

11 Figures

Supporting Text:

Site description

The mean annual precipitation, temperature and daily relative humidity at the TFP are 1230 mm, 18.2 °C and 95%, respectively. The ecosystem type at the TFP study site is a Masson Pine dominated forest, with some associated ever-green broad-leaved species. Trees were planted in the 1960s. The soil is typically mountain yellow earth (corresponding to a Haplic Acrisol in FAO). The soil is acidic, with a pH of 3.79. From previous studies, the mean Hg concentrations in precipitation, throughfall, litterfall and organic soils were 55.3 ng L^{-1}, 98.9 ng L^{-1}, 104.8±18.6 ng g^{-1} and 191 ± 65 ng g^{-1}, respectively, with an annual Hg input of 291.2 μg m^{-2} yr^{-1}.(Zhou et al., 2016;Zhou et al., 2015)

Dynamic Flux Chamber design and measurement

Semi-cylindrical quartz glass and open-bottom DFCs (4.71 L) were used during the sampling campaign. The area of the DFCs over the soil surface was 20 × 30 cm, with six inlet holes (1 cm diameter). At the outlet of the chamber, an orifice was connected to two exits; one to a regulated suction pump with a flow rate of 10 L min^{-1}, and the other to a gold cartridge for trapping outlet TGM. On the two opposite sections of the chamber, a gold trap was placed in the inlet to trap TGM entering from outside air.

Quality Assurance and Quality Control

Gold cartridges used to sample pore TGM were collected at same time as soil TGM flux measurements. All the cartridges were brought back to the laboratory at the TFP Forest Station for quantitative analysis using a cold vapor atomic fluorescence spectroscopy (CVAFS) detector (Brooks Rand III). For all Hg analysis, quality assurance and quality control (QA−QC) measures included the system blanks, gold cartridge recovery, recovery and duplicates before and after the campaign in each season. A quantitative volume of saturated Hg air at a known temperature was injected to calibrate the recovery of all gold cartridges' before and after the campaigns in each season. The recoveries of gold cartridges before and after the operation ranged from 98.8 to 103.2% and 96.3 to 102.5%, respectively. The standard deviation of the recoveries was 2.6%. Before and after field sampling, the collection efficiency of the gold quartz cartridges was detected by connecting two cartridges in sequence and sampling the ambient air for 24 h in laboratory. For all cartridges, less than 1% Hg was detected on the second cartridges compared to the first cartridge, indicating that more than 99% of TGM was absorbed by the gold cartridges during the field operation. Blanks of the soil TGM flux sampling system were routinely measured by placing the DFC on a quartz glass surface in the five plots. The sampling time of the blank measurement was same to the soil-air TGM flux measurement, which were collected twice a day: every morning (about 8:00) and

afternoon (about 17:00) representing night (17:00−8:00 of next day) and day (8:00−17:00) emissions, respectively. The averaged blank was 0.13 ± 0.21 ng m^{-2} h^{-1} (n=10), which was subtracted from the soil-air TGM flux in each season. The calibration curve was developed using Hg saturated air and had to have a correlation coefficient greater than 0.99 before the samples analysis could proceed.

Environmental measurements

Daily meteorological parameters were collected and averaged over 5-min intervals. Daily air temperature and solar radiation were monitored using a TP 101 digital thermometer and a GLZ−C photo synthetically radiometer (TOP Ltd. China), respectively, during diurnal measurements. Percent moisture was monitored with Time Domain Reflectometry (TDR) Hydra Probe II (SDI−12/RS485) and a Stevens water cable tester (USA). Measurements were taken at the same time with gold trap collection. Solar radiation was collected with a weather station (Davis Wireless Vantage VUE 06250 Weather Station, Davis Instruments, Hayward, CA) located in the TFP Forest Station about 500 m away from the sub-catchment.

For each DFC sampling location, bulk soil samples were collected from the DFC footprints (0−5 cm) in each month after the end of the measurement period. Soil samples were dried and homogenized, and completely ground to a fine powder in a pre-cleaned stainless-steel blender. The total Hg concentration in the soil samples was determined using a DMA-80 direct Hg analyzer (Milestone Ltd., Italy). SOM content in soils was determined using the sequential loss on ignition (LOI) method.(Zhou et al., 2013) A homogenized soil sample (WS) was dried at 105 ℃ for about 12- 24 h to obtain the dry weight of the samples (DW_{105}). The heated dry sample was then burned at 550 ℃ for 4 h and the weight of the sample after heating at 550 ℃ was DW_{550}. Thus, the TOM concentration (LOI_{550}) was calculated according to the following formula:

$$LOI_{550}=100(DW_{105}- DW_{550})/WS.$$

Statistical analysis

Mean pore TGM concentrations and soil TGM fluxes were compared among the five plots. Separate one-way ANOVAs were used to determine if the differences in Hg concentrations and fluxes were evident among the depths and plots. All differences in means were significant at the p=0.05 level and all means are reported with ± one standard deviation from the mean. The correlation was analyzed by Pearson's Correlation Tests using SPSS software (SPSS Inc. 16.0) and correlation coefficient and p values are presented and significantly correlated at the level of 0.05.

Table S1. Characteristics and detail of measurements at five plots in the forested sub-catchments.

Plots	Locations	Date of flux measurement				Date of soil pore TGM measurement				SOM (0-5, %)	Area (%)
		Spring	Summer	Autumn	Winter	Spring	Summer	Autumn	Winter		
Plot A	Top of the hillslope of the coniferous forest	5 Mar-7 Apr	17 -19 Jun; 1-31 Jul; 10-24 Aug	3 Nov-6 Dec	24 Dec-14 Jan	5 Mar-7 Apr	17 -19 Jun; 21-31 Jul; 10-24 Aug	3 Nov-6 Dec	24 Dec-14 Jan	13.6	42.4
Plot B	Middle of the hill slope of the coniferous forest	5 Mar-7 Apr	17 -19 Jun; 1-31 Jul; 10-24 Aug	3 Nov-6 Dec	24 Dec-14 Jan		17 -19 Jun; 21-31 Jul; 10-24 Aug	3 Nov-6 Dec	24 Dec-14 Jan	16.3	42.4
Plot C	Wetland	5 Mar-7 Apr	1-31 Jul; 10-24 Aug	3 Nov-6 Dec	31 Dec-14 Jan					4.9	2.9
Plot D	Broad-leaved forest	5 Mar-7 Apr	17 -19 Jun; 1-31 Jul; 10-24 Aug	3 Nov-6 Dec	24 Dec-14 Jan	5 Mar-7 Apr	17 -19 Jun; 21-31 Jul; 10-24 Aug	3 Nov-6 Dec	24 Dec-14 Jan	8.8	10
Plot E	Open field (deserted agricultural land)	22 Mar-7 Apr	17 -19 Jun; 1-31 Jul; 10-24 Aug	3-23 Nov	30 Dec-14 Jan		17 -19 Jun; 21-31 Jul; 10-24 Aug	3-23 Nov	30 Dec-14 Jan	4.1	2.3

98 **Table S2.** A summary of empirical models in the literature for soil-air Hg fluxes.

Parameters	Soil type	Equations	References
Temperature	Forest lake and soil	F = EXP ($-E/RT$), E is the apparent activation energy; R is the gas constant.	Xiao et al.(Xiao et al., 1991)
Temperature	Forest, open and agricultural fields.	Ln $F = E/RT + \beta_1$, E is the apparent activation energy; R is the gas constant.	Carpi and Lindberg(Carpi and Lindberg, 1997)
Temperature	Forest soil	Log $F = \beta_2 T + \beta_3$,	Xu et al.(Xu et al., 1999)
Temperature, soil Hg content	Bare soil	ln $F = -\gamma/T + \beta_4 \ln Sc + \beta_5$ γ is related to the apparent activation energy.	Gbor et al.(Gbor et al., 2006)
Solar radiation, soil Hg content	Forest soil and artificially shaded background soil	ln $F = \beta_6 L + \beta_7 \ln Sc + \beta_8$	Gbor et al.(Gbor et al., 2006)
Temperature, solar radiation	Forest soil during leaf-on period	$F = \beta_9 L + \beta_{10}$ EXP($\beta_{11} T$)	Choi and Thomas(Choi and Holsen, 2009)
Temperature	Forest soil during leaf-off period	$F = \beta_{12} + [\beta 1_3$ EXP($\beta_{14} T$ -1)]/β_{15}	Choi and Thomas(Choi and Holsen, 2009)
Temperature, solar radiation, soil moisture, Hg content	Laboratory study on background enriched Hg soil	$F = S_c \times [\beta_{16} + \beta_{17}$T + $\beta_{18} W + \beta_{19} L + \beta_{20} (T \times L) + \beta_{21} (T \times W) + \beta_{22} (W \times L) + \beta_{23} T^2 + \beta_{24} W^2 + \beta_{25} L^2]$	Lin et al.(Lin et al., 2010)
Temperature, solar radiation, Hg content	Bare soil and soil under the leaf canopy	$F = (10^{-3} \times S_c) \times [\beta_{26} + \beta_{27} T + \beta_{28} L + \beta_{29} (T \times L) + \beta_{30} T^2 + \beta_{31} L^2]$	Kikuchi et al.(Kikuchi et al., 2013)

Temperature, solar radiation, soil moisture, Hg content, atmospheric TGM	Forest soil and bare soil	$F = (a \times S_c) \times [\partial_0 + \partial_1 T + \partial_2 W + \partial_3 L + \partial_4 C_a + \partial_5 (T \times W) + \partial_6 (T \times L) + \partial_7 (T \times C_a) + \partial_8 (W \times L) + \partial_9 (W \times Ca) + \partial_{10} (L \times C_a) + \partial_{11} T^2 + \partial_{12} W^2 + \partial_{13} L^2 + \partial_{14} C_a{}^2]$	This study

β_i is the coefficients of predictors in each equations and other parameters are same in the paper.

Table S3. Coefficients of the empirical models to predicting soil-air Hg fluxes using the annual data and corresponding environmental factors of the different ecosystems.

Coefficients	Masson pine forest	Wetland	Camphor forest	Bare soil	Whole sub-catchment
∂_0	1.18	1.98	7.05×10^{-1}	1.13×10	1.39
∂_1	1.80×10^{-1}	1.39×10^{-1}	3.06×10^{-2}	-1.41	1.28×10^{-1}
∂_2	-1.13×10	-1.10	-9.24	4.48×10	-9.55
∂_3	1.05×10^{-2}	-2.37×10^{-2}	2.34×10^{-2}	2.75×10^{-3}	1.06×10^{-2}
∂_4	$-1..17\times10^{-1}$	-1.10	4.28×10^{-1}	-4.20×10^{-1}	-9.82×10^{-2}
∂_5	-1.27×10^{-1}	6.81×10^{-3}			-1.08×10^{-1}
∂_6	-2.43×10^{-4}	-1.13×10^{-4}	-5.11×10^{-4}	1.44×10^{-3}	-2.27×10^{-4}
∂_7					
∂_8				-4.91×10^{-2}	-1.13×10^{-3}
∂_9	-2.19×10^{-4}	2.55×10^{-1}	-2.61		-2.54×10^{-1}
∂_{10}				3.43×10^{-2}	7.90×10^{-7}
∂_{11}	-2.47×10^{-3}	-1.00×10^{-3}	4.19×10^{-4}	3.78×10^{-2}	-1.22×10^{-3}
∂_{12}	1.71×10		23.2×10	-1.05×10^{2}	1.44×10
∂_{13}	-4.88×10^{-5}	2.26×10^{-4}	-4.77×10^{-5}	-1.57×10^{-5}	-4.00×10^{-5}
∂_{14}		2.23×10^{-2}	3.33×10^{-2}		4.85×10^{-3}

Notes: Both first-order and second-order terms of the four factors investigated show net positive effects on the measured Hg fluxes within the data ranges of the regression analyses, and the corresponding equation is $F = (a \times S_c) \times [\partial_0 + \partial_1 T + \partial_2 W + \partial_3 L + \partial_4 C_a + \partial_5 (T\times W) + \partial_6 (T\times L) + \partial_7 (T\times C_a) + \partial_8 (W\times L) + \partial_9 (W\times Ca) + \partial_{10} (L\times C_a) + \partial_{11} T^2 + \partial_{12} W^2 + \partial_{13} L^2 + \partial_{14} C_a{}^2]$.

Table S4. Correlation coefficients of soil pore TGM concentrations in experimental plots with soil temperature, moisture and soil-air TGM fluxes for the four seasons and throughout the year.

Parameter	season	Plot A			Plot B			Plot D			Plot E		
		3	6	10	3	6	10	3	6	10	3	6	10
Soil temperature	Spr	0.37[a]	0.54[a]	0.48[a]				0.43[a]	0.09	0.13			
	Sum	0.43[a]	0.53[a]	0.40[a]	0.56[a]	0.32[b]	0.09	0.39[a]	0.42[a]	0.43[a]	0.42[a]	0.39[a]	0.34[b]
	Fall	0.46[a]	0.34[a]	0.08	0.56[a]	0.32[b]	0.09	0.32[b]	0.04	0.15	0.3[b]	0.3[b]	0.3[b]
	Win	0.25	0.45[a]	-0.01	0.34[b]	-0.06	0.34[b]	0.31[b]	0.16	0.09	0.43[b]	0.06	0
	Full year	0.85[a]	0.89[a]	0.83[a]	0.86[a]	0.74[a]	0.82[a]	0.84[a]	0.75[a]	0.67[a]	0.70[a]	0.67[a]	0.62[a]
Soil moisture	Spr	-0.18	-0.18	-0.02				-0.05	-0.05	-0.11			
	Sum	-0.22	-0.34[b]	-0.30[b]	-0.34[b]	-0.36[a]	-0.26	-0.32[b]	-0.27[b]	-0.40[a]	-0.1	-0.02	-0.16
	Fall	-0.03	0.09	-0.07	-0.34[b]	-0.36[a]	-0.26	0.03	-0.06	-0.01	-0.43[a]	-0.28	-0.28
	Win	-0.25	-0.24	0.25	0.16	0.13	0.22	-0.1	0.12	0.05	-0.28	-0.23	-0.38[b]
	Full year	-0.58[a]	-0.65[a]	-0.54[a]	-0.62[a]	-0.58[a]	-0.62[a]	-0.59[a]	-0.52[a]	-0.49[a]	-0.47[a]	-0.41[a]	-0.41[a]
Exchange fluxes	Spr	0.59[a]	0.41[a]	0.26[b]				0.49[a]	0.24	0.34[a]			
	Sum	0.42[a]	0.45[a]	0.36[a]	0.42[a]	0.26	0.18	0.51[a]	0.52[a]	0.27[b]	0.71[a]	0.59[a]	0.64[a]
	Fall	0.37[b]	0.35[a]	-0.12	0.42[a]	0.26	0.18	0.50[a]	0.12	0.09	0.33[b]	0.13	0.13
	Win	0.57[a]	0.53[a]	0.18	0.64[a]	-0.46[a]	0.25	0.51[a]	0.29	0.47[a]	0.65[a]	0.38[b]	0.3
	Full year	0.64[a]	0.65[a]	0.55[a]	0.72[a]	0.64[a]	0.67[a]	0.63[a]	0.51[a]	0.36[a]	0.77[a]	0.69[a]	0.65[a]

[a] Correlation is significant at the 0.01 level (two-tailed); [b] Correlation is significant at the 0.05 level (two-tailed). Note that soil temperature and moisture were directly determined in surface soil by Time Domain Reflectometry (TDR) with a Stevens water cable tester, not in each layer.

Figure Captions:

Fig. S1. The study area of the study area.(Wang et al., 2017)

Fig. S2. Correlation between the averaged solar radiation (8: 0-17:00) and daily soil-air Hg flux measured as the average of day and night values for the five plots.

Fig. S3. Effects of precipitation events on soil-air TGM fluxes at the five plots for the four seasons and annually.

Fig. S4. Correlation between the soil Hg concentrations ($S_c \pm SD$) and soil-air Hg flux ($F \pm SD$) under the forest canopy. Standard deviations of soil Hg concentrations were obtained from Hg concentrations in the four seasons (n=12). Because fluxes are often controlled by solar radiation for bare soils, the correlation analysis above does not include the open field (plot E).

Fig. S5. Correlation between the soil temperature and daily soil-air Hg flux measured as the average of day and night values for the five plots.

Fig. S6. Correlation between the soil moisture and daily soil-air Hg flux measured as the average of day and night values for the five plots.

Fig. S7. Correlation between the air TGM concentration and daily soil-air Hg flux measured as the average of day and night values for the five plots.

Fig. S8. Scatterplots of model-predicted and DFC-measured fluxes between soil and air in the Masson pine (a), wetland (b), camphor (c) and open field (d) plots.

Fig. S9. Hg (a) and TOM concentrations (b) with the soil depth at the collection depths of soil pore TGM.

Fig. S10. Correlation between the gradient of TGM concentrations between soil pore (3 cm) and atmosphere values and soil-air TGM flux at the four plots.

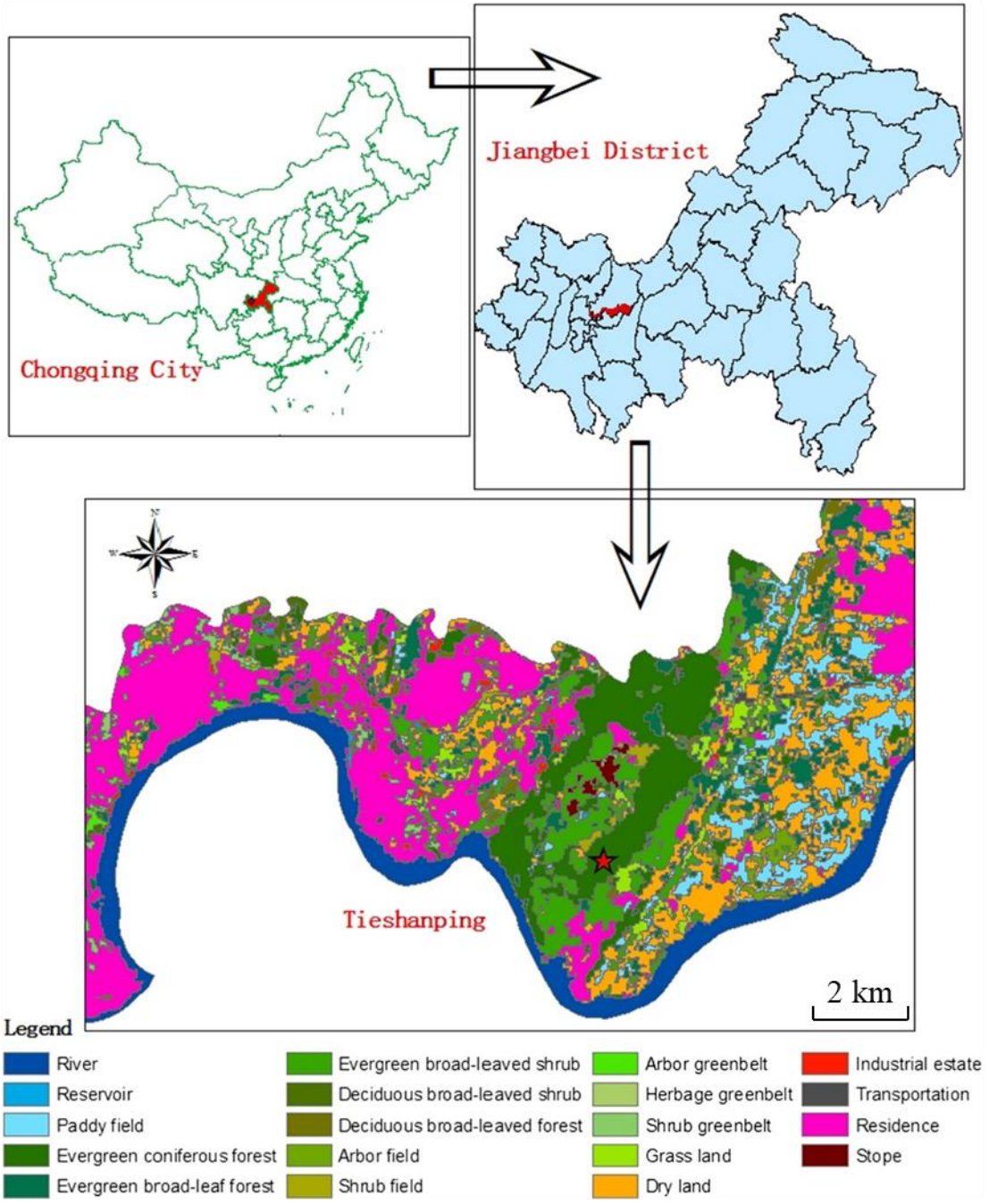

137

138 **Fig. S1**. The study area of the study area.(Wang et al., 2017)

139

140

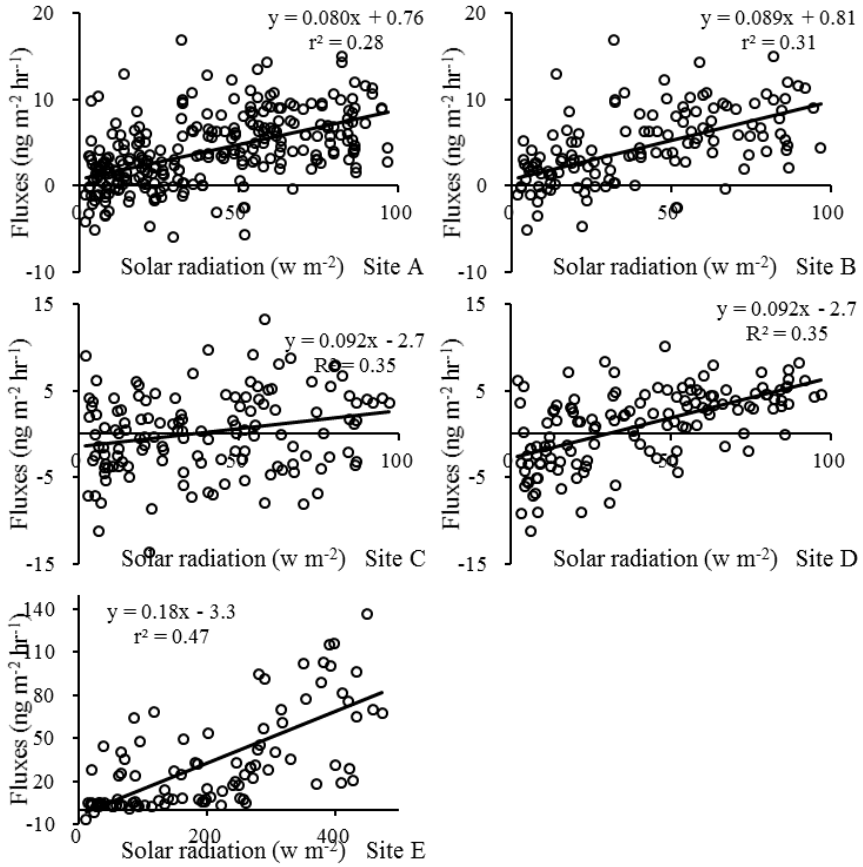

141

142

143 **Fig. S2.** Correlation between the averaged solar radiation (8: 0-17:00) and daily soil-air Hg flux
144 measured as the average of day and night values for the five plots.

145

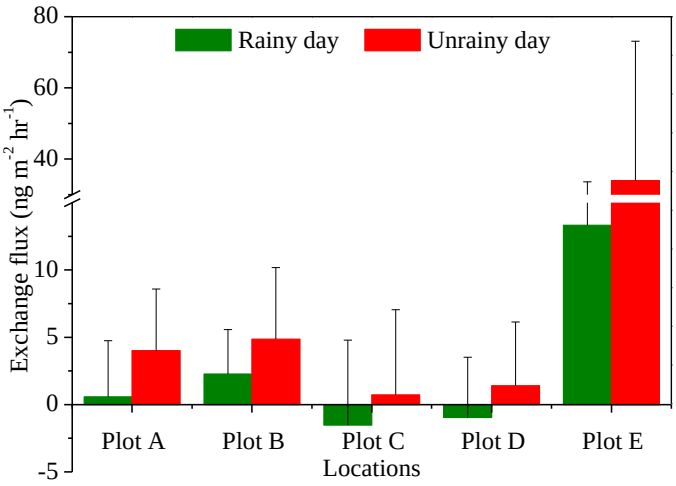

Fig. S3. Effects of precipitation events on soil-air TGM fluxes at the five plots for the four seasons and annually.

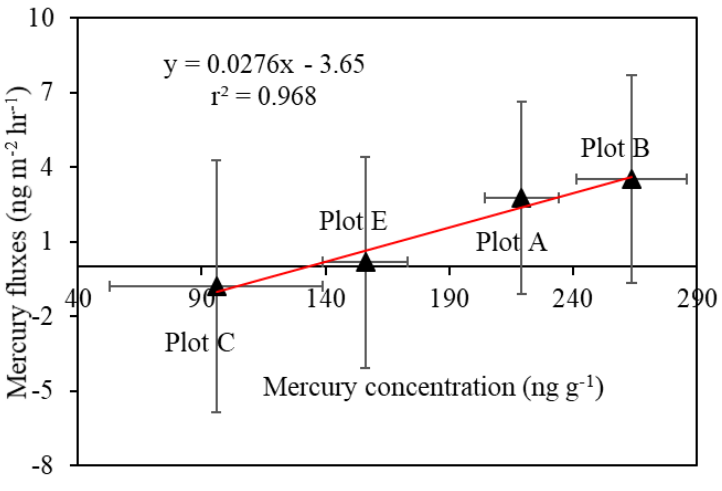

Fig. S4. Correlation between the soil Hg concentrations ($S_c \pm SD$) and soil-air Hg flux ($F \pm SD$) under the forest canopy. Standard deviations of soil Hg concentrations were obtained from Hg concentrations in the four seasons (n=12). Because fluxes are often controlled by solar radiation for bare soils, the correlation analysis above does not include the open field (plot E).

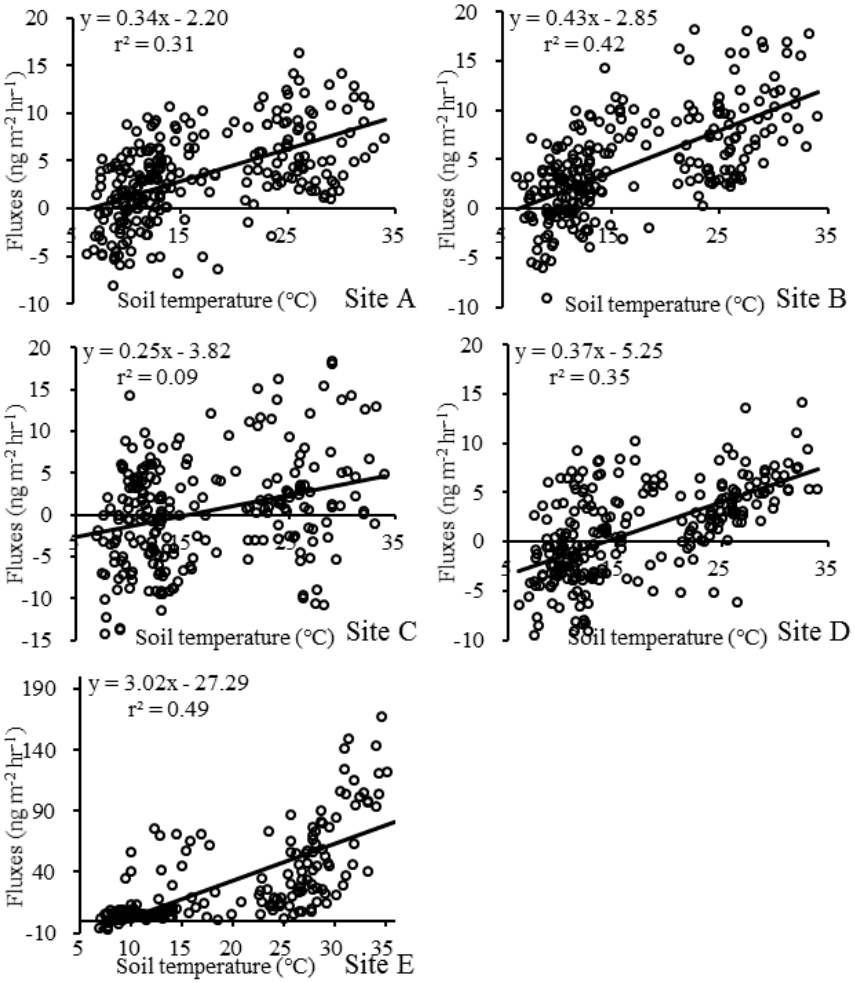

Fig. S5. Correlation between the soil temperature and daily soil-air Hg flux measured as the average of day and night values for the five plots.

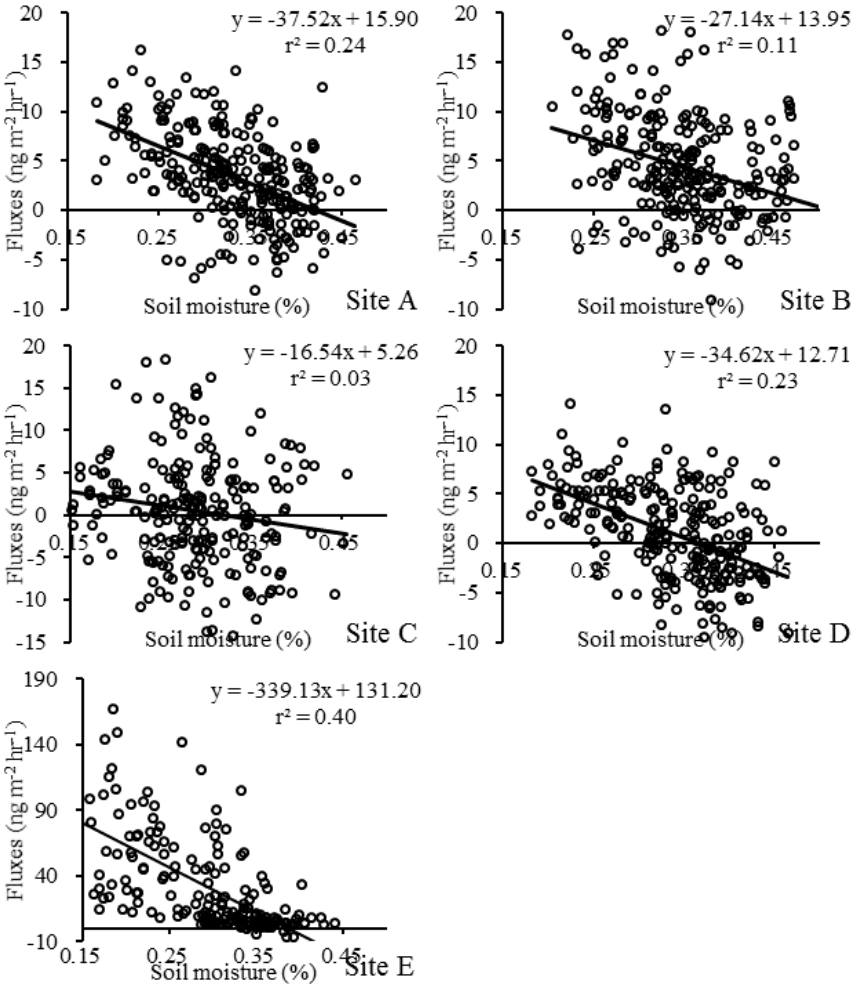

Fig. S6. Correlation between the soil moisture and daily soil-air Hg flux measured as the average of day and night values for the five plots.

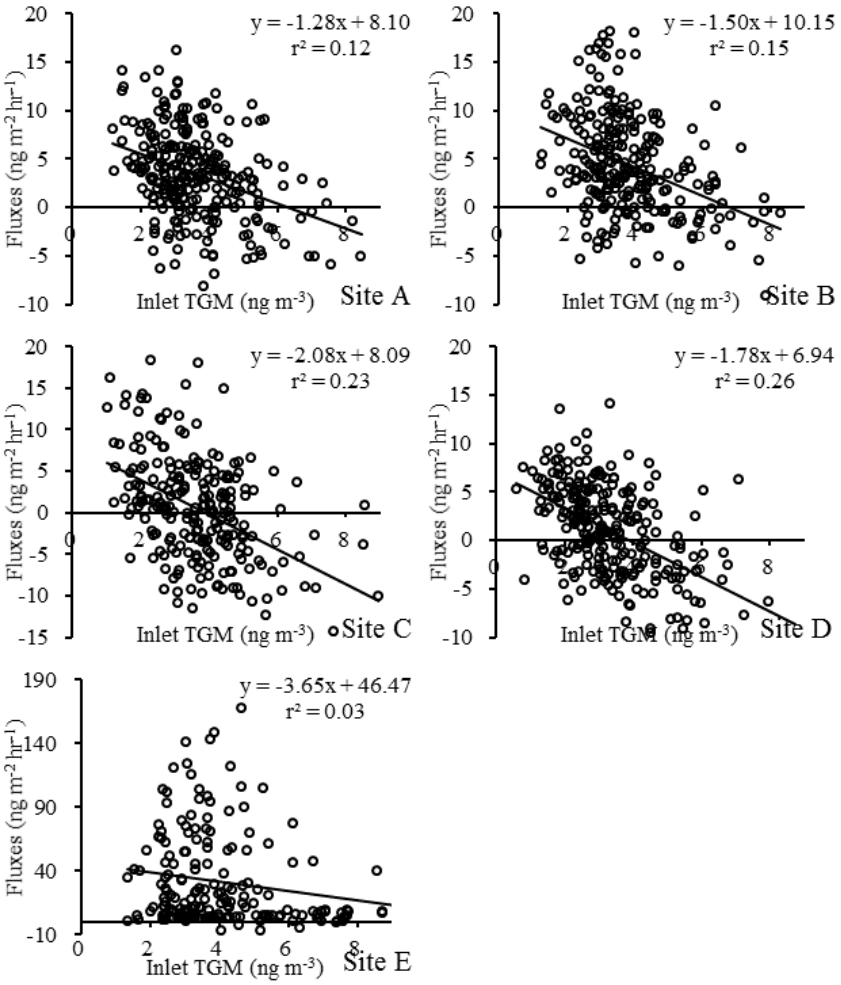

Fig. S7. Correlation between the air TGM concentration and daily soil-air Hg flux measured as the average of day and night values for the five plots.

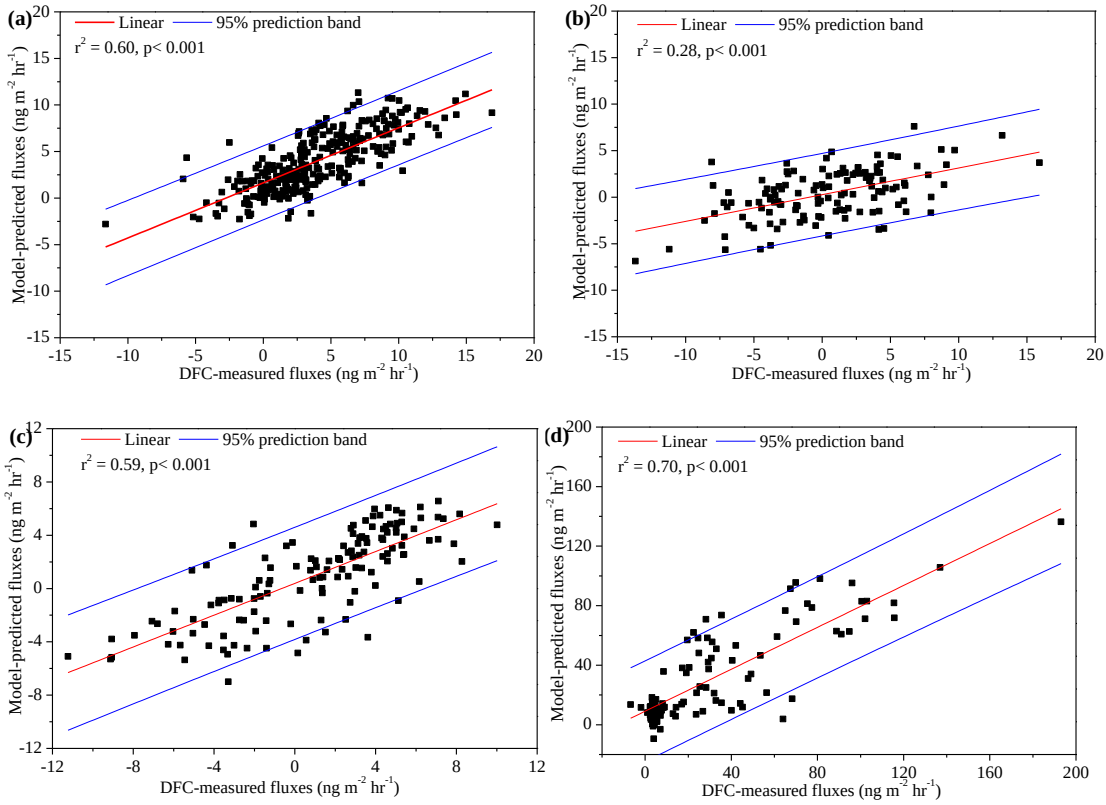

Fig. S8. Scatterplots of model-predicted and DFC-measured fluxes between soil and air in the Masson pine (a), wetland (b), camphor (c) and open field (d) plots.

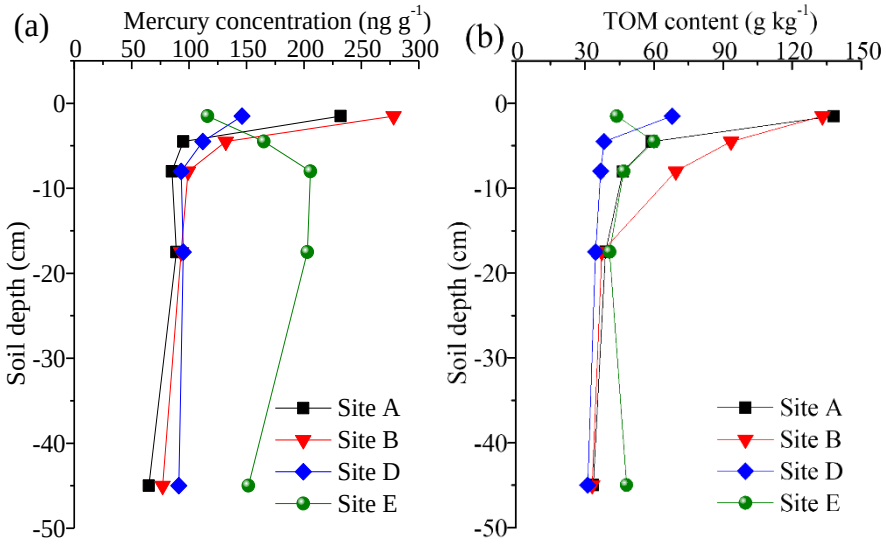

Fig. S9. Hg (a) and TOM concentrations (b) with the soil depth at the collection depths of soil pore TGM.

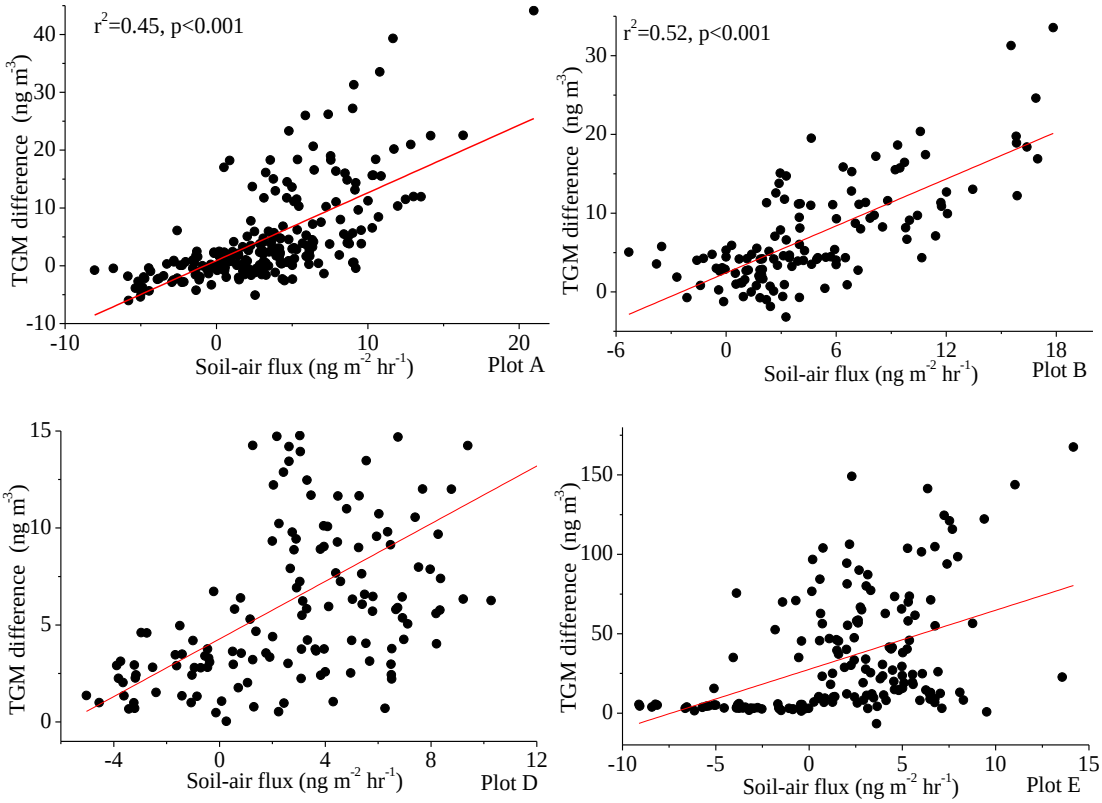

184

185

186 **Fig. S10.** Correlation between the gradient of TGM concentrations between soil pore (3 cm) and
187 atmosphere values and soil-air TGM flux at the four plots.

188

References:

Carpi, A., and Lindberg, S. E.: Sunlight-mediated emission of elemental mercury from soil amended with municipal sewage sludge, Environmental Science & Technology, 31, 2085-2091, 1997.

Choi, H.-D., and Holsen, T. M.: Gaseous mercury emissions from unsterilized and sterilized soils: The effect of temperature and UV radiation, Environmental pollution, 157, 1673-1678, 10.1016/j.envpol.2008.12.014, 2009.

Gbor, P. K., Wen, D., Meng, F., Yang, F., Zhang, B., and Sloan, J. J.: Improved model for mercury emission, transport and deposition, Atmospheric Environment, 40, 973-983, 2006.

Kikuchi, T., Ikemoto, H., Takahashi, K., Hasome, H., and Ueda, H.: Parameterizing soil emission and atmospheric oxidation-reduction in a model of the global biogeochemical cycle of mercury, Environmental Science & Technology, 47, 12266-12274, 2013.

Lin, C. J., Gustin, M. S., Singhasuk, P., Eckley, C., and Miller, M.: Empirical models for estimating mercury flux from soils, Environmental Science & Technology, 44, 8522-8528, 2010.

Wang, J., Zhang, X., Wang, Z., and Kang, R.: A relative method for measuring nitric oxide (NO) fluxes from forest soils, Science of the Total Environment, 574, 544-552, 10.1016/j.scitotenv.2016.09.012, 2017.

Xiao, Z. F., Munthe, J., Schroeder, W. H., and Lindqvist, O.: Vertical fluxes of volatile mercury over forest soil and lake surfaces in Sweden, Tellus Series B-Chemical and Physical Meteorology, 43, 267-279, 10.1034/j.1600-0889.1991.t01-1-00001.x, 1991.

Xu, X., Yang, X., Miller, D. R., Helble, J. J., and Carley, R. J.: Formulation of bi-directional atmosphere-surface exchanges of elemental mercury, Atmospheric Environment, 33, 4345-4355, 1999.

Zhou, J., Feng, X., Liu, H., Zhang, H., Fu, X., Bao, Z., Wang, X., and Zhang, Y.: Examination of total mercury inputs by precipitation and litterfall in a remote upland forest of Southwestern China, Atmospheric Environment, 81, 364-372, 10.1016/j.atmosenv.2013.09.010, 2013.

Zhou, J., Wang, Z., Zhang, X., and Chen, J.: Distribution and elevated soil pools of mercury in an acidic subtropical forest of southwestern China, Environmental pollution, 202, 187-195, 10.1016/j.envpol.2015.03.021, 2015.

Zhou, J., Wang, Z., Sun, T., Zhang, H., and Zhang, X.: Mercury in terrestrial forested systems with highly elevated mercury deposition in southwestern China: The risk to insects and potential release from wildfires, Environmental pollution, 212, 188-196, 10.1016/j.envpol.2016.01.003, 2016.